

# Immunoassays on Thiol-Ene Synthetic Paper Generate a Superior Fluorescence Signal

Weijin Guo<sup>a</sup>, Lluisa Vilaplana<sup>bc</sup>, Jonas Hansson<sup>a</sup>, M.-Pilar Marco<sup>bc</sup>, and Wouter van der Wijngaart<sup>\*a</sup>

<sup>a</sup> KTH Royal Institute of Technology, Micro and Nanosystems, Malvinas väg 10, 100 44 Stockholm, Sweden.

<sup>b</sup> Nanobiotechnology for diagnostics (Nb4D), Department of Surfactants and Nanobiotechnology, Institute for Advanced Chemistry of Catalonia (IQAC) of the Spanish Council for Scientific Research (CSIC), Jordi Girona 18-26, 08034 Barcelona, Spain

<sup>c</sup> CIBER de Bioingeniería, Biomateriales y Nanomedicina (CIBER-BBN), Jordi Girona 18-26, 08034 Barcelona, Spain

\*Corresponding author. Email: [wouter@kth.se](mailto:wouter@kth.se)

**Abstract**

1 The fluorescence-based detection of biological complexes on solid substrates is widely used in  
2 microarrays and lateral flow tests. Here, we investigate thiol-ene micropillar scaffold sheets  
3 ("synthetic paper") as the solid substrate in such assays. Compared to state-of-the-art glass and  
4 nitrocellulose substrates, assays on synthetic paper provide a stronger fluorescence signal, similar  
5 or better reproducibility, lower limit of detection (LOD), and the possibility of working with  
6 lower immunoreagent concentrations. Using synthetic paper, we detected the antibiotic  
7 enrofloxacin in whole milk with a LOD of 1.64 nM, which is on par or better than the values  
8 obtained with other common tests, and much lower than the maximum level allowed by European  
9 Union regulations. The significance of these results lays in that they indicate that synthetically-  
10 derived microstructured substrate materials have the potential to improve the performance of  
11 diagnostic assays.

12  
13 Keywords: biosensor, enrofloxacin, fluorescence, glass slides, microarray, nitrocellulose, off-  
14 stoichiometric thiol-ene, porous substrate

## 1. Introduction

Many molecular sensor formats use solid surfaces as assay substrates, for example bead-based assays, lateral flow devices and microarrays. Typical substrate materials include glass, nitrocellulose and polymers. Glass substrates have a very low autofluorescence and support a range of well-established surface modification methods[1, 2, 3, 4]. Nitrocellulose substrates allow biomolecule immobilisation by passive absorption and are used where no easy immobilization by covalent chemical conjugation is available[5] or where their high surface area enables a large colorimetric signal. Polymer substrates are typically used in microfluidic immunoassays where they provide a compromise between ease of fabrication, integration, function, surface modification and cost[6].

The geometric structure of the substrate material influences the performance of the test. Flat surfaces, such as those of glass slides, have a very controlled geometry and are easy to rinse, which helps in keeping the variability and low background of the readout signal low. Porous surfaces, such as nitrocellulose, provide a large binding area but are difficult to rinse efficiently, helping in an increased readout signal but with high variability and background.

Here, we investigate “synthetic paper”[7], a micropillar scaffold made of off-stoichiometric thiolene (OSTE)[8], as a substrate for fluorescence-based sensors. The porosity of synthetic paper is lithographically defined and therefore very well controlled. The pore size is tunable, and typically of size tens to hundred of  $\mu\text{m}$ , which we hypothesize can allow for efficient rinsing (low background). The surface area per footprint is typically several times higher than that of flat surfaces, which we hypothesize allows for a high readout signal. Furthermore, synthetic paper features reactive thiol groups on its native surface, which readily enables covalent biomolecule binding.

The performance of a given substrate material (readout signal, reproducibility, variance, specificity) depends largely on the specific assay. Our aim is to indicate the potential of synthetic paper as a substrate for molecular sensing, and we do this by setting up an immunoassay in a

microarray format for the detection of a relevant biomarker: enrofloxacin. We compare synthetic paper with - traditionally used - glass[3] and nitrocellulose[5] as the substrate in fluorescent microarrays for the detection of enrofloxacin in milk. Enrofloxacin is one member of fluoroquinolones, a class of broad-spectrum antibiotics widely used for the prevention and treatment of diseases in humans and animals[9, 10, 11]. However, the extensive use of enrofloxacin may induce antibiotic resistance[12], which can spread to humans through the food chain[13]. To protect the public health, maximum residue levels (MRLs) of enrofloxacin have been defined by the European Union[14, 15, 16]. For detection of fluoroquinolones in animal tissue or milk, the available methods include high performance liquid chromatography (HPLC), liquid chromatography-mass spectrometry (LC-MS)[17, 18, 19, 20], and immunochemical detection (ELISA[21, 22], lateral flow test strips[23, 24], electrochemical sensors[25], surface plasmon resonance sensors[26, 27]). To our best knowledge, fluorescent microarrays have not been used for enrofloxacin detection in milk.

## **2. Material and methods**

### **2.1. Materials, chemicals and biochemicals**

Glass slides were purchased from Corning Inc (Corning, NY, USA). Nitrocellulose slides were bought from ArrayIt<sup>®</sup> corporation (Catalog ID: SMN, Sunnyvale, CA, USA). The microstructuring resin Ostemer 220, used for synthetic paper fabrication, was provided by Mercene Labs (Stockholm, Sweden). Preda-BSA which is a fluoroquinolone haptenized protein conjugate[31], was provided by the Custom Antibody Service (CAbS, CIBER-BBN, IQAC, CSIC). Sulfo-SMCC (sulfosuccinimidyl 4-(N-maleimidomethyl)cyclohexane-1-carboxylate, ThermoFisher SCIENTIFIC, USA) was used as a cross-linking reagent that reacts with amino and sulfhydryl groups. To quantify proteins, we used Bradford protein assay dye reagent concentrate from Bio-Rad (Hercules, California, USA). We used Bovine serum albumin (Sigma Life Science, Germany), milk powder (Nestle milk company, Spain), Polyvinylpyrrolidone (Sigma-Aldrich, USA), and gelatin (Sigma, Canada) for surface blocking of substrates. Anti-Mouse IgG (whole

molecule) - TRITC antibody produced in goat (T5393-1ML, Sigma-Aldrich, USA) was used as the secondary antibody. Whole milk was from Grupo Lactalis (Lleida, Spain). Phosphate buffer saline (PBS) is phosphate buffer (0.01 M) in a 0.8% saline solution at pH 7.5. PBST means PBS with 0.05% Tween 20. The immunoreagents used in the experiments are very stable when kept under appropriate conditions (lyophilized or frozen).

## 2.2. Equipment and general procedures

The fabrication process of synthetic paper can be found in the Appendix. Briefly, we fabricated the synthetic paper in  $\sim 10\text{ cm} \times \sim 10\text{ cm}$  sheets using Ostemer 220, after which we cut the synthetic paper sheets in pieces compatible with the microarray system using a xurograph (Cutting Plotter CE5000-60, Graphtech). We wetted the synthetic paper surface with PBST, washed it with DI water and blow-dried it with nitrogen gas.

Glass slides were washed with piranha solution ( $\text{H}_2\text{SO}_4\text{:H}_2\text{O}_2$ , 70:30) for 30 min, followed by DI water rinsing. Subsequently they were activated with 10% NaOH solution (Carlo Erba Reagents S.A.S, Italy) for 30 min, and rinsed with DI water.[4] After drying, we used 3-glycidyloxypropyltrimethoxysilane (GPTMS) (300  $\mu\text{L}$ /slide, 30 min) to functionalize the glass slide surface[4]. After silanization, we washed the slides again with ethanol, dried them and stored them in a desiccator for later use.

Bioconjugates were characterized by MALDI-TOF/TOF-MS (Billerica, Massachusetts, USA), comparing the molecular weight of the unreacted protein with those of the conjugate, thus allowing to calculate hapten densities. To perform these analysis, we used 4  $\mu\text{L}$  of matrix mixture (trans-3,5-dimethoxy-4-hydroxycinnamic acid, 10 mg/mL in Acetonitrile/ $\text{H}_2\text{O}$  70:30, 0.1%  $\text{HCOOH}$ ) and the bioconjugates at the volume ratio 1:1. The density of the maleimide groups incorporated was estimated using the equation  $[\text{MW}(\text{Preda-BSA-Maleimide}) - \text{MW}(\text{Preda-BSA})]/\text{MW}[\text{maleimide group}]$  (details in Appendix). Printing of the bioconjugate (Preda-BSA and Preda-BSA-maleimide) spots on all the substrates was done using a BioOdyssey Calligrapher

MiniArrayer (Bio-Rad Laboratories, Inc., Hercules, CA, USA). All the experiments on microarray systems were done on an ArrayIt® holder.

### 2.3. Fluorescence signal measurement

Measurement of the fluorescence signal of the substrates was done with a ScanArray Gx PLUS (PerkinElmer, Waltham, MA, USA). The fluorescence signal information was obtained from the software ScanArray Express v 4.0 (Microarray Analysis System, PerkinElmer, Waltham, MA, USA). The fluorescence signal was determined as the difference between the average intensity of the spots and the background intensity. GraphPad Prism 5 (GraphPad Software Inc., San Diego, CA, USA) was used to obtain the competitive curves from experimental results using the equation  $Y = [(A - B)/(1 + (x/C)^D)] + B$ , in which A refers to the maximal fluorescence intensity, B to the minimum fluorescence intensity, C to the value IC<sub>50</sub>, i.e., the concentration producing 50% of the difference between A and B, and D to the absolute value of the slope of the sigmoid curve at the inflection point.

### 2.4. Conjugation of Preda-BSA

15 µL Sulfo-SMCC solution (34.65 mg/mL in dimethylformamide, 1.19 µmol Sulfo-SMCC in total) were added dropwise to 640 µL Preda-BSA solution (4.219 mg/mL in PBS, 0.04 µmol Preda-BSA in total), and mixed for 4 hours in a 3 mL glass vial using a magnetic stirrer. After stirring, we transferred the solution to a 1.5 mL plastic tube. We centrifuged the solution for 7 min at 4000 rpm, and took the upper clear solution. After that, we used a HiTrap Desalting column (Sigma-Aldrich, USA) for the separation of the new bioconjugate: Preda-BSA-maleimide from bioconjugate of Preda-BSA and Sulfo-SMCC following the standard protocol. The concentration of the bioconjugate was determined to be 0.91 mg/mL using the Bradford protein assay test.

### 2.5. Fluorescent microarray experiments

We used the capillary pin MCP310S in all spotting experiments. 8 × 3 microarray regions were printed on each one of the synthetic papers tested and on glass slides or nitrocellulose slides. Within each region, 3 lines with 5 spots per line were spotted. Each spot was dispensed two times.

For an optimal and accurate comparison between the substrates, we first determined the best bioconjugate concentration, primary antibody concentration and surface blocking strategy for each of the substrates as shown in Fig. 2c. To obtain the optimal curve, at first we performed 2D checkerboard experiments to determine the best coating antigen and primary antibody concentrations (Fig. A10). After that, we performed optimization experiments (changing pH of the buffers, and tween concentrations) to improve the  $IC_{50}$  if needed. Compared to glass and nitrocellulose slides, synthetic paper needed less amount of primary antibody, which means lower cost on the immunoassay.

To perform the immunoassay, we spotted the conjugate Preda-BSA as coating antigen on nitrocellulose and glass slides, and Preda-BSA-maleimide on synthetic paper slides. The surface bounding chemistry is covalent between maleimido groups and thiol groups on synthetic paper, and also covalent between amino groups and epoxy groups on glass, while the bounding on nitrocellulose is by passive absorption.

After spotting, we transferred all the slides to the spotter chamber, where they were kept overnight. Thereafter, we fixed the slides on the ArrayIt<sup>®</sup> holder, and a silicon gasket was used to define  $8 \times 3$  wells on each slide. After that, we washed each well ( $3 \times$  PBST). Subsequently, a blocking step was performed by adding 100  $\mu$ L 1% gelatin solution (in PBS) in each well, followed by 30 min incubation, after which the slides were washed ( $3 \times$  PBST).

50  $\mu$ L of enrofloxacin solution (in PBST, 20% milk in DI water, or milk) was added in each well, immediately followed by the addition of 50  $\mu$ L of primary antibody (in PBST with  $CaCl_2$  (Sigma, USA), the concentration of  $CaCl_2$  is 1 mM). After 30 min incubation, a washing step was performed ( $3 \times$  PBST). As standard curve, we tested different enrofloxacin concentrations: 2  $\mu$ M, 200 nM, 64 nM, 20 nM, 10 nM, 2 nM, 0.2 nM, and 0 nM, which were prepared by serial dilution of the analyte.

Next, we added 100  $\mu$ L of secondary antibody (1/250 in PBST) in each well and incubated during 30 min. After this, the slides were washed ( $3 \times$  PBST and  $1 \times$  DI water). The slides were dried

using nitrogen gas, and the fluorescence signal was measured with the scanner. Due to the strong background noise of nitrocellulose slide, for this substrate specifically we changed the imaging settings to obtain a high signal-to-noise ratio while avoiding saturation. The operating temperature of this experiment was 20 °C.

### 3. Results and Discussion

We perform this study by comparing synthetic paper with - traditionally used - glass[3] and nitrocellulose[5] as the substrate in fluorescent microarrays for the detection of enrofloxacin in milk.

Compared with HPLC and LC-MS methods, microarrays do not need bulky equipment and experienced technicians; compared to ELISA, microarrays can have similar sensitivity but lower cost[28, 29, 30], and allow the detection of different analytes easily (multiplex) and even the detection of analytes of different chemical nature (proteins and DNA in multimodal assays); compared to lateral flow test, microarrays reach lower LODs, and; compared to electrochemical and surface plasmon resonance sensors, microarrays require less complex fabrication.

We investigated the performance of different synthetic paper variants as fluorescence microarray substrates by comparing their performance with those of the well-established glass and nitrocellulose substrates. We fabricated three synthetic paper (SP) substrate variants with differences in micropillar diameter,  $d$ ; scaffold pitch,  $p$ ; and substrate thickness,  $t$ : SP1 ( $d = 50\ \mu\text{m}$ ,  $p = 100\ \mu\text{m}$ ,  $t = 100\ \mu\text{m}$ ); SP2 ( $d = 50\ \mu\text{m}$ ,  $p = 100\ \mu\text{m}$ ,  $t = 200\ \mu\text{m}$ ); SP3 ( $d = 25\ \mu\text{m}$ ,  $p = 50\ \mu\text{m}$ ,  $t = 100\ \mu\text{m}$ ) (Fig. 1). We choose these dimensions because they combine easy fabrication and sufficient surface area for the application.

We used the detection of enrofloxacin in PBST with an indirect competitive assay in a microarray format as a validation assay to test the performance of the new synthetic papers (Fig. 1)[31]. We performed the assay on all the substrates on the same day, repeated the experiments 3 times on different days, and compared their performance (Fig. 2). To allow for a fair comparison, an optimisation was performed for the blocking agent concentration, bioconjugate concentration and

primary antibody concentration for each of the five substrates separately (Fig. 2c). The imaging settings of the scanner were the same for all the substrates tested, except for nitrocellulose slides because of their strong autofluorescence.

The  $IC_{50}$  values obtained are slightly higher than those reported for Elisa assays (1.8 nM)[31, 32]. Synthetic papers showed lower  $IC_{50}$  values than nitrocellulose slides (17.98 nM) and glass slides (12.78 nM). Among the synthetic papers, SP2 (4.02 nM) performs slightly better than SP3 (6.52 nM) and SP1 (11.04 nM). The LOD values of the substrates show a similar trend as the  $IC_{50}$  values, as can be expected. The fitting of a sigmoidal curve to the measurement data was excellent for all substrates (worst for nitrocellulose with  $R^2=0.9559$ , best for glass with  $R^2=0.9979$ , and 0.99 or higher for all synthetic papers). The variance in fluorescent signal was low for the glass slides (3.5%), SP2 (5.4%) and SP1 (5.6%), and substantially higher for SP3 (9.8%) and nitrocellulose (14.6%). In terms of substrate reproducibility, glass performs best with a slope variance of 3.2%, synthetic papers have slope variance between 4% and 5%, while that of nitrocellulose is 10.3%. We ascribe the low variance of glass to the low autofluorescence and the flatness (i.e. no microstructure on the surface, which makes it easier to focus when imaging). We suspect that the high variation for SP3 and nitrocellulose result from their small pore size, which makes removal of unbounded molecules from those substrates during washing steps less efficient. The high surface area of SP3 and nitrocellulose explain the high fluorescence intensities for these substrates. The widest measurement range (from 2.22 to 19.19 nM) was obtained for SP3.

Compared to glass slides, synthetic papers have stronger fluorescent signal, lower  $IC_{50}$  and lower LOD (due to their higher surface area) but slightly higher variation (due to their microstructure). The fluorescent signal intensity from SP2 is  $\sim 2$  times higher than that from glass slides, which can be advantageous when measuring sensitive fluorescent molecules by allowing a reduction of exposure time. Compared to nitrocellulose slide, synthetic papers have lower  $IC_{50}$ , lower LOD, and lower variation (due to their larger pore size making washing more efficient). Among the three different kinds of synthetic paper, SP1 and SP2 have the same pillar diameter and pitch-to-

pitch distance, but the thickness of SP2 is double that of SP1, which means that SP2 has 1.70 times bigger surface area than SP1. Their performance is similar in terms of signal variance, reproducibility, goodness of fit, and the amount of bioconjugate and primary antibody, whereas SP2 has slightly lower  $IC_{50}$  and LOD values. SP1 and SP3 have the same thickness, but the pillar diameter and pitch-to-pitch distance of SP3 are half those of SP1. Their performance is similar in terms of  $IC_{50}$ , LOD and goodness of fit, but SP3 needs less amount of bioconjugate and primary antibody (which means lower cost of the immunoassay), but has a higher variation.

Considering the overall good performance of SP2, we tested this substrate for the detection of enrofloxacin in whole milk (Fig. 3). As overviewed in Table 1, we obtained an LOD value of 1.64 nM and an  $IC_{50}$  value of 8.62 nM, i.e., much lower than required by EU regulation[14]. The  $IC_{50}$  value is on par with that of electrochemical sensing[33] and surface plasmon resonance immunosensing[26], but lower than that in wavelength-interrogated optical sensing[34].

To study the effect of the matrix we compared the assays run in PBST, diluted whole milk (whole milk:DI water = 1:5), and whole milk (Fig. 3). We performed the assay in all buffers on the same day, repeated the experiments 3 times on different days, and compared their performance (Fig. 3). The effect of whole milk was not significant when compared to PBST. Performing the assay in 1:5 diluted milk resulted in a lower LOD and a wider measurement range. We hypothesize that milk blocks the synthetic paper surface from unspecific reactions.

To test the accuracy of the assay, we measured the fluorescence intensity of blind spiked milk samples with different enrofloxacin concentrations (4, 8, 16, 24, 32, 40, 48, 96, 192  $\mu\text{g/mL}$ ). We used the previously obtained sigmoidal curve to deduce the concentration. Plotting the deduced concentration against the original concentration shows a regression line with slope close to 1 and an  $R^2$  larger than 0.95 (Fig. 3c). The recovery ratio of enrofloxacin is shown in Supplementary Information (Table A1).

#### 4. Conclusions

We have investigated synthetic paper as a synthetic substrate with large pore size for fluorescent microarrays. Due to its unique surface chemistry, low autofluorescence, and large and well-controlled pores, synthetic paper resulted in a stronger fluorescence intensity and lower limit of detection compared to nitrocellulose slides. Due to its increased surface area per footprint, synthetic paper resulted in a stronger fluorescence intensity compared to glass slide substrates. We further showed that different synthetic paper geometries provided different signal responses. Our results thus support our research hypothesis that surfaces with controlled microstructure porosity can improve the biosensor performance.

Furthermore, compared to NC and glass, synthetic paper required lower amounts of primary antibody, a driver of cost for many bioassays.

We successfully ran indirect competitive assays to detect enrofloxacin - an important target in the milk industry – reaching a low limit of detection. We were able to measure enrofloxacin directly in whole milk, indicating that our system should allow the detection of this antibiotic in real samples at significant concentrations.

Because the design of this study required the resource-intensive optimization of assays for three different substrates separately, we limited ourselves to the study of one assay. These first results, however, encourage future efforts for the development of synthetic paper as a substrate for multiplex antibiotics detection, for use of detection of other types of analyte, or for use in fluorescence-based lateral flow tests.

#### **Declaration of interests**

Co-author Jonas Hansson is employed at Mercene Labs who holds the patent rights on synthetic paper. The other authors declare that they have no known competing financial interests or personal relationships that could have appeared to influence the work reported in this paper.

#### **CRedit authorship statement**

Weijin Guo: Investigation, Methodology, Formal analysis, Data curation, Visualization, Writing - original draft. Lluisa Vilaplana: Conceptualization, Methodology, Writing - Review Editing, Supervision. Jonas Hansson: Methodology, Writing - Review Editing, Supervision. M.-Pilar Marco: Conceptualization, Funding acquisition, Methodology, Supervision. Wouter van der Wijngaart: Conceptualization, Funding acquisition, Methodology, Writing - review editing, Supervision.

## Acknowledgments

We gratefully acknowledge the financial support from the European project ND4ID, and Ministry of Science, Innovation and Universities Spain (IMMUNO-QS, SAF2015-67476-R and QS4CF, RTI2018-096278-B-C21). We thank Dr Ana Sanchis from IQAC-CSIC for providing the glass slides and assistance in operating the spotter and scanner, Dr David Santos for the MALDI-TOF tests, and Dr Nuria Pascual for providing the primary antibodies.

## References

- [1] S. Nagl, M. Schaeferling, O. S. Wolfbeis, Fluorescence analysis in microarray technology, *Microchimica Acta* 151 (2005) 1–21.
- [2] H. B. Pollard, M. Srivastava, O. Eidelman, C. Jozwik, S. W. Rothwell, G. P. Mueller, D. M. Jacobowitz, T. Darling, W. B. Guggino, J. Wright, et al., Protein microarray platforms for clinical proteomics, *PROTEOMICS–Clinical Applications* 1 (2007) 934–952.
- [3] J. B. Delehanty, F. S. Ligler, A microarray immunoassay for simultaneous detection of proteins and bacteria, *Analytical Chemistry* 74 (2002) 5681–5687.

- 1 [4] A. Sanchis, J.-P. Salvador, K. Campbell, C. T. Elliott, W. L. Shelver, Q. X. Li, M.-P. Marco,  
2 Fluorescent microarray for multiplexed quantification of environmental contaminants in seawater  
3 samples, *Talanta* 184 (2018) 499–506.
- 4 [5] D. Wang, S. Liu, B. J. Trummer, C. Deng, A. Wang, Carbohydrate microarrays for the  
5 recognition of cross-reactive molecular markers of microbes and host cells, *Nature biotechnology*  
6 20 (2002) 275.
- 7 [6] L. Mou, X. Jiang, Materials for microfluidic immunoassays: a review, *Advanced healthcare*  
8 *materials* 6 (2017) 1601403.
- 9 [7] J. Hansson, H. Yasuga, T. Haraldsson, W. Van der Wijngaart, Synthetic microfluidic paper:  
10 high surface area and high porosity polymer micropillar arrays, *Lab on a Chip* 16 (2016) 298–304.
- 11 [8] C. F. Carlborg, T. Haraldsson, K. Öberg, M. Malkoch, W. van der Wijngaart, Beyond pdms:  
12 off-stoichiometry thiol–ene (oste) based soft lithography for rapid prototyping of microfluidic  
13 devices, *Lab on a Chip* 11 (2011) 3136–3147.
- 14 [9] J. Hernández-Arteseros, J. Barbosa, R. Compano, M. Prat, Analysis of quinolone residues in  
15 edible animal products, *Journal of Chromatography A* 945 (2002) 1–24.
- 16 [10] Y. Zhu, L. Li, Z. Wang, Y. Chen, Z. Zhao, L. Zhu, X. Wu, Y. Wan, F. He, J. Shen,  
17 Development of an immunochromatography strip for the rapid detection of 12 fluoroquinolones in  
18 chicken muscle and liver, *Journal of agricultural and food chemistry* 56 (2008) 5469–5474.
- 19 [11] Y. Zhao, G. Zhang, Q. Liu, M. Teng, J. Yang, J. Wang, Development of a lateral flow  
20 colloidal gold immunoassay strip for the rapid detection of enrofloxacin residues, *Journal of*  
21 *agricultural and food chemistry* 56 (2008) 12138–12142.

- [12] J.M. Nelson, T.M. Chiller, J. H. Powers, F. J. Angulo, Fluoroquinolone-resistant campylobacter species and the withdrawal of fluoroquinolones from use in poultry: a public health success story, *Clinical Infectious Diseases* 44 (2007) 977–980.
- [13] B. M. Marshall, S. B. Levy, Food animals and antimicrobials: impacts on human health, *Clinical microbiology reviews* 24 (2011) 718–733.
- [14] F. Fernández, D. G. Pinacho, M. Gratacós-Cubarsí, J.-A. García- Regueiro, M. Castellari, F. Sánchez-Baeza, M.-P. Marco, Immunochemical determination of fluoroquinolone antibiotics in cattle hair: A strategy to ensure food safety, *Food chemistry* 157 (2014) 221–228.
- [15] C. Regulation, No 470/2009 of the european parliament and of the council of 6 may 2009 laying down a community procedures for the establishment of residue limits of pharmacologically active substances in foodstuffs of animal origin, repealing council regulation (eec) no 2377/90 and amending directive 2001/82, *Official Journal of the European Union L* 152 (2009) 11–22.
- [16] H. REGULATION, Council regulation (eec) no 2377/90 of 26 june 1990 laying down a community procedure for the establishment of maximum residue limits of veterinary medicinal products in foodstuffs of animal origin, *Official JL* 224 (1990) 0001–0008.
- [17] M. Hermo, D. Barrón, J. Barbosa, Development of analytical methods for multiresidue determination of quinolones in pig muscle samples by liquid chromatography with ultraviolet detection, liquid chromatography–mass spectrometry and liquid chromatography–tandem mass spectrometry, *Journal of Chromatography A* 1104 (2006) 132–139.
- [18] M. Hermo, E. Nemutlu, S. Kır, D. Barrón, J. Barbosa, Improved determination of quinolones in milk at their mrl levels using lc–uv, lc–fd, lc–ms and lc–ms/ms and validation in line with regulation 2002/657/ec, *Analytica chimica acta* 613 (2008) 98–107.

- [19] S. Zhao, H. Jiang, X. Li, T. Mi, C. Li, J. Shen, Simultaneous determination of trace levels of 10 quinolones in swine, chicken, and shrimp muscle tissues using hplc with programmable fluorescence detection, *Journal of agricultural and food chemistry* 55 (2007) 3829–3834.
- [20] E. A. Christodoulou, V. F. Samanidou, I. N. Papadoyannis, Development of an hplc multi-residue method for the determination of ten quinolones in bovine liver and porcine kidney according to the european union decision 2002/657/ec, *Journal of separation science* 31 (2008) 119–127.
- [21] S. Bucknall, J. Silverlight, N. Coldham, L. Thorne, R. Jackman, Antibodies to the quinolones and fluoroquinolones for the development of generic and specific immunoassays for detection of these residues in animal products, *Food Additives & Contaminants* 20 (2003) 221–228.
- [22] A.-C. Huet, C. Charlier, S. A. Tittlemier, G. Singh, S. Benrejeb, P. Delahaut, Simultaneous determination of (fluoro) quinolone antibiotics in kidney, marine products, eggs, and muscle by enzyme-linked immunosorbent assay (elisa), *Journal of agricultural and food chemistry* 54 (2006) 2822–2827.
- [23] Z. Peng, Y. Bang-Ce, Small molecule microarrays for drug residue detection in foodstuffs, *Journal of Agricultural and Food Chemistry* 54 (2006) 6978–6983.
- [24] C. Cháfer-Pericás, A. Maquieira, R. Puchades, Fast screening methods to detect antibiotic residues in food samples, *TrAC Trends in Analytical Chemistry* 29 (2010) 1038–1049.
- [25] G. E. Pellegrini, G. Carpico, E. Coni, Electrochemical sensor for the detection and presumptive identification of quinolone and tetracycline residues in milk, *Analytica chimica acta* 520 (2004) 13–18.

- [26] F. Fernández, K. Hegnerová, M. Piliarik, F. Sanchez-Baeza, J. Homola, M.-P. Marco, A label-free and portable multichannel surface plasmon resonance immunosensor for on site analysis of antibiotics in milk samples, *Biosensors and Bioelectronics* 26 (2010) 1231–1238.
- [27] F. Fernández, D. G. Pinacho, F. Sánchez-Baeza, M. P. Marco, Portable surface plasmon resonance immunosensor for the detection of fluoroquinolone antibiotic residues in milk, *Journal of agricultural and food chemistry* 59 (2011) 5036–5043.
- [28] P. R. Knight, A. Sreekumar, J. Siddiqui, B. Laxman, S. Copeland, A. Chinnaiyan, D. G. Remick, Development of a sensitive microarray immunoassay and comparison with standard enzyme-linked immunoassay for cytokine analysis, *Shock* 21 (2004) 26–30.
- [29] K. L. Jenko, Y. Zhang, Y. Kostenko, Y. Fan, C. Garcia-Rodriguez, J. Lou, J. D. Marks, S. M. Varnum, Development of an elisa microarray assay for the sensitive and simultaneous detection of ten biodefense toxins, *Analyst* 139 (2014) 5093–5102.
- [30] C. Desmet, L. J. Blum, C. A. Marquette, Multiplex microarray elisa versus classical elisa, a comparison study of pollutant sensing for environmental analysis, *Environmental Science: Processes & Impacts* 15 (2013) 1876–1882.
- [31] D. G. Pinacho, F. Sánchez-Baeza, M.-P. Marco, Molecular modeling assisted hapten design to produce broad selectivity antibodies for fluoroquinolone antibiotics, *Analytical chemistry* 84 (2012) 4527–4534.
- [32] J. Adrian, D. G. Pinacho, B. Granier, J.-M. Diserens, F. Sánchez-Baeza, M.-P. Marco, A multianalyte elisa for immunochemical screening of sulfonamide, fluoroquinolone and  $\beta$ -lactam antibiotics in milk samples using class-selective bioreceptors, *Analytical and Bioanalytical Chemistry* 391 (2008) 1703–1712.

- [33] D. G. Pinacho, F. Sánchez-Baeza, M.-I. Pividori, M.-P. Marco, Electrochemical detection of fluoroquinolone antibiotics in milk using a magneto immunosensor, *Sensors* 14 (2014) 15965–15980.
- [34] J. Adrian, S. Pasche, G. Voirin, D. G. Pinacho, H. Font, F. Sánchez-Baeza, M.-P. Marco, J.-M. Diserens, B. Granier, Wavelength-interrogated optical biosensor for multi-analyte screening of sulfonamide, fluoroquinolone,  $\beta$ -lactam and tetracycline antibiotics in milk, *TrAC Trends in Analytical Chemistry* 28 (2009) 769–777.

## Figures

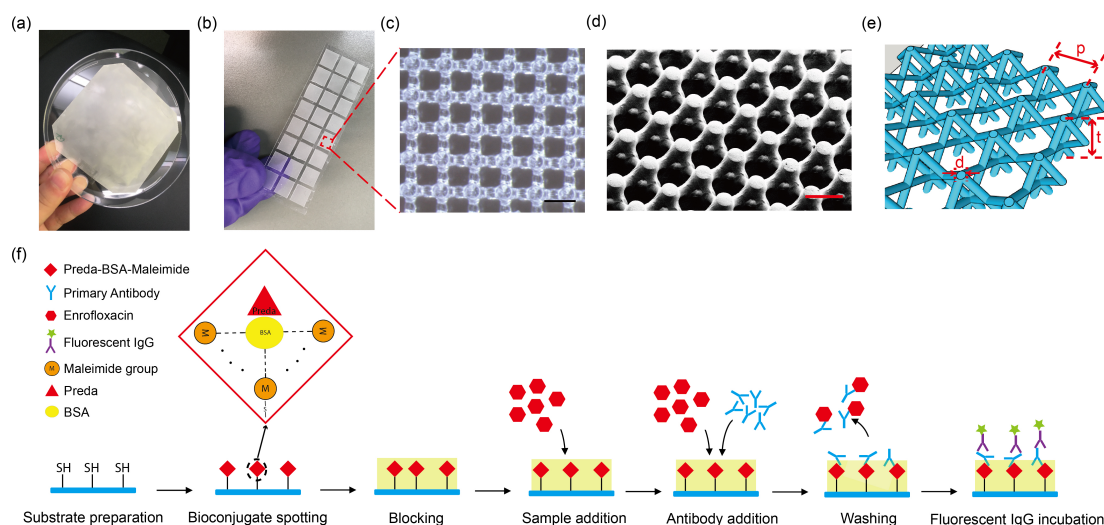


**Fig.1.** Synthetic paper (a-e) and scheme of the immunoassay (f). (a) Photograph of a  $10 \times 10 \text{ cm}^2$  sheet of synthetic paper in a large petri dish. (b) Photograph of the synthetic paper after cutting in a format suitable for microarray assays. (c) Top view bright field microscopy image of synthetic paper (scale bar  $100 \mu\text{m}$ ). (d) A SEM picture of synthetic paper (scale bar  $100 \mu\text{m}$ ). (e) Schematic perspective view of synthetic paper.  $d$  is the micropillar diameter,  $p$  is the scaffold pitch, and  $t$  is the substrate thickness. Scheme of the competitive fluorescence immunoassay (f), which consists of substrate preparation, spotting of bioconjugate, gelatin blocking, competition step: addition of the analyte followed by adding the specific primary antibody, washing, and incubation with the fluorescent secondary antibody. During the spotting, the maleimide group from the bioconjugate reacts with the thiol group on the synthetic paper. There are  $\sim 12$  maleimide groups on one single Preda-BSA molecule (see Appendix for measurement and calculations).

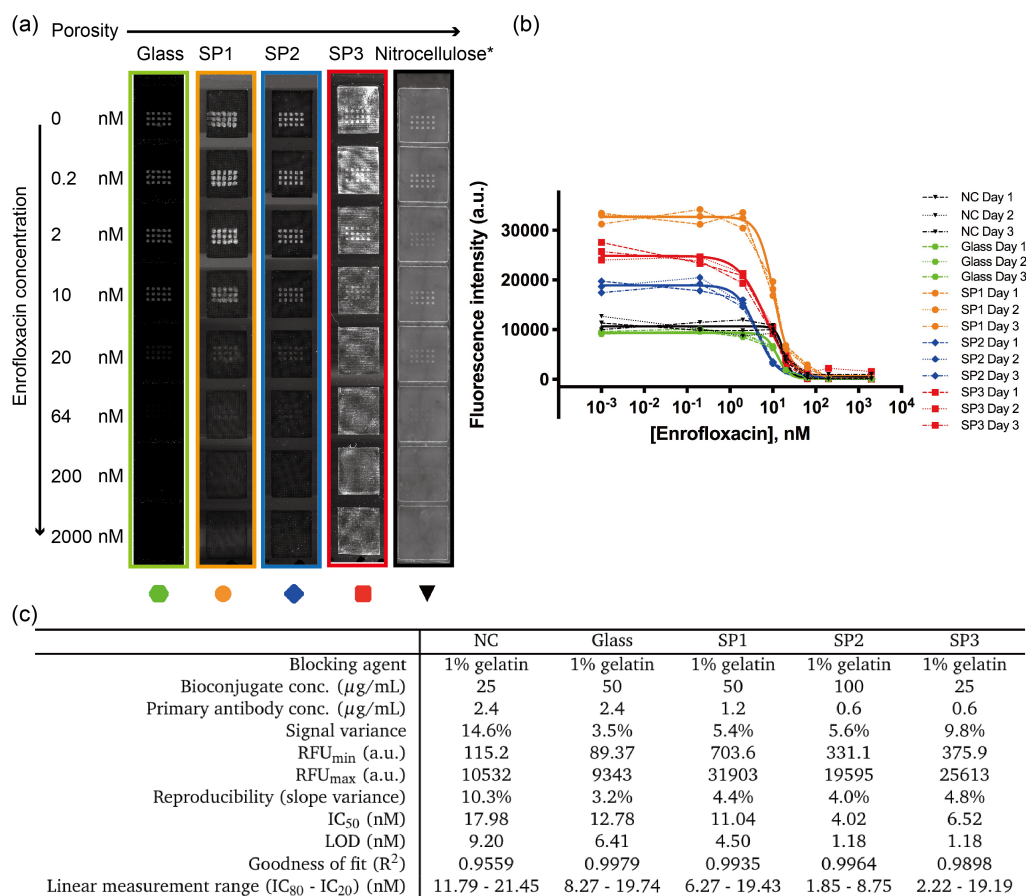


**Fig.2.** Microarray performance comparing different substrates. Three synthetic papers (SP) with different architecture have been tested together with glass and nitrocellulose (NC) slides. a) Indirect competitive assay to detect serial enrofloxacin dilutions. The fluorescence signal obtained for each substrate is shown. The same gain and power have been used for glass and SPs. For NC slides, the gain and power were reduced. b) Calibration curves (dots) obtained for each substrate. Dashed, dotted and dash-dotted lines connect measurements acquired on the same day. The solid line indicates the sigmoidal curve fit to the average measurement value. c) Analytical parameters of the fluorescent microarrays on all the substrates tested. The signal variance is the variance in fluorescence intensity for spots from an assay run on a given day, i.e., the coefficient of variation standard deviation / average,  $N = 15$ ; the reproducibility is the variance of the slope value of the sigmoid curve from assays run on different days, i.e., standard deviation / average,  $N = 3$ ; RFU<sub>min</sub> and RFU<sub>max</sub> are the respective minimum and maximum measured relative fluorescence units; IC<sub>50</sub> is the concentration producing 50% of inhibition of the maximal fluorescence signal; the LOD is the IC<sub>90</sub> value, defined as the concentration producing 90% of the maximal fluorescence signal; the goodness of fit is the squared error  $R^2$  between the measurements of the standard serial dilutions and the sigmoid curve fit, and; the linear measurement range of the sensor is defined as IC<sub>80</sub> to IC<sub>20</sub>, where IC<sub>20</sub> is the concentration producing the fluorescence intensity 80% of

- 1 the minimum plus 20% of the maximum and IC<sub>80</sub> is the concentration producing fluorescence intensity 80% of the
- 2 maximum plus 20% of the minimum.

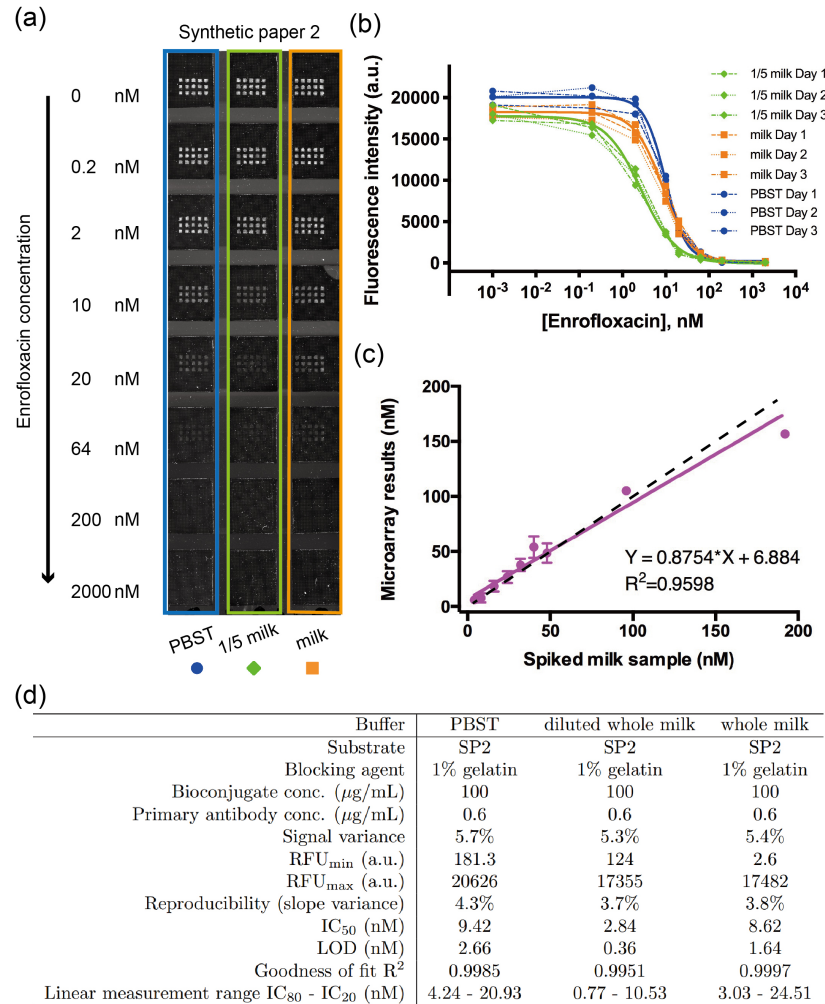


**Fig.3.** Detection of enrofloxacin in whole milk on synthetic paper 2 (SP2). a) Indirect competitive assay to detect serial enrofloxacin dilutions. From left to right, serial dilutions of enrofloxacin were prepared in PBST, 1/5 diluted milk , milk. b) Calibration curves (dots) obtained for each substrate. Dashed, dotted and dash-dotted lines connect measurements acquired on the same day. The solid line indicates the sigmoidal curve fit to the average measurement value. c) The solid line is the fitting line between blind spiked and measured concentration values. The dashed line refers to the perfect correlation (slope = 1). N = 3. d) Analytical parameters of the fluorescent protein microarrays on SP2 tested. The signal variance is the variance in fluorescence intensity for spots from an assay run on a given day, i.e., the coefficient of variation standard deviation / average, N = 15; the reproducibility is the variance of the slope value of the sigmoid curve from assays run on different days, i.e., standard deviation / average, N = 3; RFU<sub>min</sub> and RFU<sub>max</sub> are the respective minimum and maximum measured relative fluorescence units; IC<sub>50</sub> is the concentration producing 50% of inhibition of the maximal fluorescence signal; the LOD is the IC<sub>90</sub> value, defined as the concentration producing 90%

of the maximal fluorescence signal; the goodness of fit is the squared error  $R^2$  between the measurements of the standard serial dilutions and the sigmoid curve fit, and; the linear measurement range of the sensor is defined as  $IC_{80}$  to  $IC_{20}$ , where  $IC_{20}$  is the concentration producing the fluorescence intensity 80% of the minimum plus 20% of the maximum and  $IC_{80}$  is the concentration producing fluorescence intensity 80% of the maximum plus 20% of the minimum.

Table 1. Comparison of  $IC_{50}$  and LoD value

Enrofloxacin detection	Our method	Maxim residue levels of EU regulation [14]*	Electrochemical magneto immunosensor [33]	Surface plasmon resonance immunosensor [26]	Wavelength-interrogated optical sensing [34]
<b><math>IC_{50}</math> (nM)</b>	8.62	N.A.	5.68	8.93	83.75
<b>LoD (nM)</b>	1.64	288.98	N.A.	0.83	5.56

\* We transfer the unit from ug/kg to nM, by assuming the milk density is 1035 kg/m<sup>3</sup>.  
N.A. means not available.